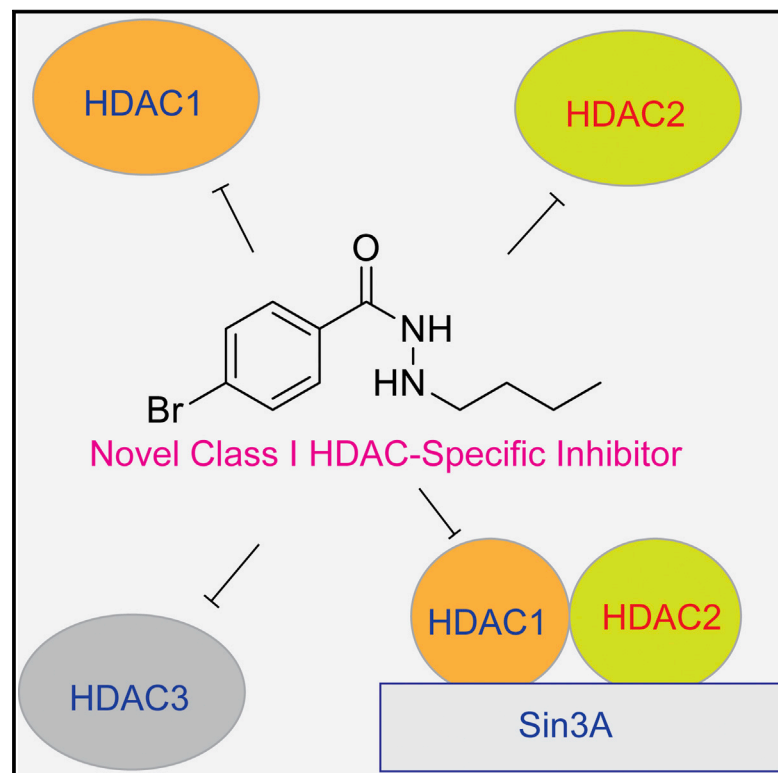


# Chemistry & Biology

## Identification of Histone Deacetylase Inhibitors with Benzoylhydrazide Scaffold that Selectively Inhibit Class I Histone Deacetylases

### Graphical Abstract



### Authors

Yunfei Wang, Ryan L. Stowe, ..., William R. Roush, Daiqing Liao

### Correspondence

dliao@ufl.edu

### In Brief

Class I HDACs are therapeutic targets. Entinostat, specific to these HDACs, improves treatment outcome for advanced breast cancer, but toxicity and poor drug properties may hamper its clinical applications. Wang et al. report a benzoylhydrazide group of class I HDAC-selective inhibitors that may overcome some of these limitations.

### Highlights

- Discovery of class I HDAC-selective inhibitors with a new benzoylhydrazide scaffold
- Nanomolar inhibition potencies against HDACs 1–3 by UF010 analogs
- HDAC inhibition potency correlates with their cytotoxicity to cancer cells
- UF010 activates tumor suppression mechanisms while inhibiting oncogenic pathways

### Accession Numbers

GSE56823



# Identification of Histone Deacetylase Inhibitors with Benzoylhydrazide Scaffold that Selectively Inhibit Class I Histone Deacetylases

Yunfei Wang,<sup>1,2</sup> Ryan L. Stowe,<sup>3</sup> Christie E. Pinello,<sup>5</sup> Guimei Tian,<sup>1</sup> Franck Madoux,<sup>5</sup> Dawei Li,<sup>1,7</sup> Lisa Y. Zhao,<sup>1,9</sup> Jian-Liang Li,<sup>6</sup> Yuren Wang,<sup>8</sup> Yuan Wang,<sup>8</sup> Haiching Ma,<sup>8</sup> Peter Hodder,<sup>4,5,10</sup> William R. Roush,<sup>3</sup> and Daiqing Liao<sup>1,\*</sup>

<sup>1</sup>Department of Anatomy and Cell Biology, UF Health Cancer Center and UF Genetics Institute, University of Florida College of Medicine, Gainesville, FL 32610, USA

<sup>2</sup>Department of Biochemistry and Molecular Biology, College of Life Sciences, Northwest Agriculture and Forestry University, Yangling, Shaanxi 712100, China

<sup>3</sup>Department of Chemistry, Scripps Florida, Jupiter, FL 33458, USA

<sup>4</sup>Department of Molecular Therapeutics, Scripps Florida, Jupiter, FL 33458, USA

<sup>5</sup>The Scripps Research Institute Molecular Screening Center, Lead Identification Division, Translational Research Institute, Scripps Florida, Jupiter, FL 33458, USA

<sup>6</sup>Sanford-Burnham Medical Research Institute at Lake Nona, Orlando, FL 32827, USA

<sup>7</sup>Department of Urology, Qilu Hospital, Shandong University, Jinan, Shandong 250012, China

<sup>8</sup>Reaction Biology Corporation, 1 Great Valley Parkway Suite 2, Malvern, PA 19355, USA

<sup>9</sup>Present address: Department of Medicine, University of Florida College of Medicine, Gainesville, FL 32610, USA

<sup>10</sup>Present address: Amgen Inc., One Amgen Center Drive, Thousand Oaks, CA 91320-1799, USA

\*Correspondence: [dliao@ufl.edu](mailto:dliao@ufl.edu)

<http://dx.doi.org/10.1016/j.chembiol.2014.12.015>

## SUMMARY

Inhibitors of histone deacetylases (HDACi) hold considerable therapeutic promise as clinical anti-cancer therapies. However, currently known HDACi exhibit limited isoform specificity, off-target activity, and undesirable pharmaceutical properties. Thus, HDACi with new chemotypes are needed to overcome these limitations. Here, we identify a class of HDACi with a previously undescribed benzoylhydrazide scaffold that is selective for the class I HDACs. These compounds are competitive inhibitors with a fast-on/slow-off HDAC-binding mechanism. We show that the lead compound, UF010, inhibits cancer cell proliferation via class I HDAC inhibition. This causes global changes in protein acetylation and gene expression, resulting in activation of tumor suppressor pathways and concurrent inhibition of several oncogenic pathways. The isotype selectivity coupled with interesting biological activities in suppressing tumor cell proliferation support further preclinical development of the UF010 class of compounds for potential therapeutic applications.

## INTRODUCTION

Histone deacetylases (HDACs) remove the acetyl group from lysine residues of histones and other cellular proteins. HDACs are classified into four phylogenetic groups: class I (HDAC1, HDAC2, HDAC3, and HDAC8), class II (HDAC4, HDAC5, HDAC7, and HDAC9 in the class IIa subgroup, and HDAC6

and HDAC10 in the IIb subgroup), class III (Sirt1 to Sirt7), and class IV (HDAC11) (Smith et al., 2008; Yang and Seto, 2008). Classes I, IIb, and IV HDACs possess bona fide Zn<sup>2+</sup>-dependent acetyl-lysine deacetylase activities. While heightened HDAC activities are implicated in several disorders, including chronic neurologic, inflammatory, and metabolic conditions (Christensen et al., 2014; Fass et al., 2013; Wagner et al., 2013), abnormal epigenetic regulation, including globally or locally altered patterns of histone acetylation, has long been implicated in cancer etiology and progression. In particular, the roles of HDAC1, HDAC2, and HDAC3 in promoting cancer progression have been extensively documented (Muller et al., 2013; New et al., 2012; Wilson et al., 2006).

Chemically diverse classes of small-molecule inhibitors of HDACs (HDACi) have been developed and characterized, and many exhibit potent anticancer properties in preclinical and clinical studies (Bolden et al., 2006; Bradner et al., 2010). Based on the structures of the Zn<sup>2+</sup>-chelating chemical groups, HDAC inhibitors can be divided into four major classes: hydroxamic acids, aminobenzamides, cyclic peptides, and aliphatic acids. A variety of derivatives of each class have been synthesized and characterized. Three compounds, vorinostat and belinostat (hydroxamic acids) and romidepsin (a cyclic peptide), have been approved for clinical anticancer therapies (Marks, 2010; New et al., 2012). These US Food and Drug Administration (FDA)-approved drugs and a number of other HDACi have undergone clinical evaluations for treating a variety of hematological malignancies and solid tumors (New et al., 2012).

However, there are a number of issues that may limit broad clinical utility of the currently known HDAC inhibitors. Hydroxamic acids are pan-HDACi, active against different isoforms of HDACs, and feature a rather strong Zn<sup>2+</sup>-chelating group (warhead), which is also found in inhibitors of other metalloenzymes, such as matrix metalloproteases (MMPs) and tumor

necrosis factor alpha-converting enzyme (DasGupta et al., 2009; Lotsch et al., 2013; Nuti et al., 2011), although a recent study shows that metal-chelating drugs generally do not display overt off-target activities (Day and Cohen, 2013). This raises the risk of significant off-target activities and unpredictable clinical toxicity. Although several mechanisms such as the induction of apoptosis, cell-cycle arrest, or inhibition of DNA repair are proposed to account for the antineoplastic activities of HDACi, it remains challenging to determine precisely the importance of HDAC inhibition for anticancer effects using pan-HDACi due to off-target activities. Although yet to be proven, it is generally thought that HDACi with increased isoform selectivity and potency would be safer agents with reduced side effects and could lead to superior clinical outcomes, because such selective compounds would target only HDAC activities that are dysregulated in a particular type of cancer without causing unnecessary toxicity stemming from inhibiting other HDAC isoforms. Thus, there have been significant efforts in drug development to identify HDACi with greater isozyme specificity (Ononye et al., 2012). The aminobenzamide class of HDACi is selective to class I HDACs (HDACs 1–3) and displays unique slow-on/slow-off HDAC-binding kinetics (Beconi et al., 2012; Chou et al., 2008; Lauffer et al., 2013; Newbold et al., 2013). A number of these compounds, such as MS-275 (entinostat), have been tested in clinical trials to treat diverse types of human cancer (Gojo et al., 2007; Martinet and Bertrand, 2011). However, a recent study reports that aminobenzamides seem to exhibit intrinsic liabilities, including chemical instability under certain conditions, high in vivo metabolic turnover, and efficient removal by P-glycoprotein drug transporters, which may significantly hamper their potential clinical utility (Beconi et al., 2012). Although cyclic peptides are more potent against the class I HDACs (Bradner et al., 2010), the sulfhydryl group of romidepsin is thought to chelate zinc with little specificity (Arrowsmith et al., 2012). Moreover, serious adverse events associated with cyclic peptides, including cardiac toxicity, have been reported (Martinet and Bertrand, 2011). These observations call for the development of potent and isoform-selective HDACi of novel chemotypes to overcome these limitations in order to unleash the considerable therapeutic potentials of pharmacological HDAC inhibition.

Through a high-throughput screening (HTS) effort, we discovered a lead compound that selectively inhibits HDAC1, HDAC2, and HDAC3 of the class I HDACs. This lead compound (**UF010**) features a previously unknown benzoylhydrazide scaffold as the HDACi pharmacophore. Initial structure-activity relationship (SAR) studies confirm the critical components of this scaffold for HDAC inhibition. Importantly, HDAC inhibition potency of **UF010** and analogs correlates with their ability to impair cancer cell proliferation. In addition, **UF010** alters global gene expression to activate antineoplastic pathways. Thus, this new class of HDACi can serve as powerful tools to investigate roles of HDACs in the biology of human diseases.

## RESULTS

### HTS Identification of HDACi with Novel Chemotypes

To discover small-molecule HDACi with novel chemotypes, we conducted an HTS campaign of 622,360 compounds using the Scripps Drug Discovery Library. For the primary screen, we en-

gineered a luciferase reporter under the control of the adenovirus (Ad) major late promoter (*Ad-MLP-Luc*) in the colon cancer HCT116 cell line. Compared with the luciferase reporter under the control of the Ad *E2* early promoter (*Ad-E2-Luc*), the *Ad-MLP-Luc* reporter activity dramatically increased in a dose-dependent manner by HDACi vorinostat or MS-275 (Figure S1). The similar responses of the *Ad-MLP-Luc* reporter to different classes of HDACi indicate that HDAC inhibition is the primary mechanism for the reporter activation. Each library compound was assayed at a single point and a single dose (8.6  $\mu$ M). The reporter activity was detected as luminescence readout, and cell viability was monitored with PrestoBlue dye as fluorescence intensity in a multiplex format (Figure S2). A viability counterscreen assay was used to remove highly toxic compounds. The HTS assays were robust with  $Z'$  of > 0.6 (Figure S3). A specific hit cutoff based on an average plus 3-fold SD was applied, resulting in the identification of 5,868 compounds, which increased the *Ad-MLP-Luc* activity by 9.2% of the high control (vorinostat at 28  $\mu$ M). These compounds were tested in confirmation assays in triplicate at 8.6  $\mu$ M, among which 1,575 compounds were confirmed to activate the *Ad-MLP-Luc* reporter (Figure S3). The top 637 compounds were further tested in 10-point dose-response assays in triplicate in the *Ad-MLP-Luc* activation assay (Figure S3). We then selected 315 compounds highly active in the cell-based assays for in vitro HDAC1 inhibition assays using the HDAC-Glo I/II reagents (Figure S4). A majority (54%) of these compounds inhibited HDAC1 in vitro with a potency of <10  $\mu$ M, among which there were nine hydroxamates, including vorinostat and scriptaid, and seven aminobenzamides (Figure S6A). These results highlight the robustness of the cell-based *Ad-MLP-Luc* activation assays for identifying HDACi with significant inhibitory properties.

In subsequent studies, we focused on hits with novel chemical scaffolds. A confirmed hit with a benzoylhydrazide scaffold (**UF010**) displayed consistent HDAC inhibition in biochemical and cell-based assays. We profiled **UF010** against all  $Zn^{2+}$ -dependent HDACs and found that **UF010** is class I HDAC selective with nanomolar potencies against HDACs 1–3 (Table 1).

### SAR of UF010 and Analogs

**UF010** was resynthesized and its activities were confirmed. A total of >50 **UF010** analogs with a variety of modifications of the benzoylhydrazide scaffold have been synthesized and their activities determined (data for select analogs are shown in Table 2). These SAR data indicate that a tripartite structure of this scaffold with a central  $-C(O)-NH-NH-$  unit flanked by a phenyl group and a short aliphatic chain is important for HDAC inhibition. The short 4-carbon linear aliphatic chain appears nearly optimal (Table 2). Any changes in the chain length (increase or decrease) or structure (e.g., branched) reduced HDAC inhibition potency. As for the phenyl group, the presence of a relatively bulky substituent at the *para* position relative to the carbonyl group seems critical for HDAC inhibition (Table 2). Among the analogs we have examined thus far, three (**SR-3208**, **-3302**, and **-3459**) displayed improved potencies versus HDACs 1–3 (Table 2).

We have performed comparative molecular modeling studies of **UF010** and the new analogs by using the Schrödinger modeling package. This docking study was performed without

**Table 1. Inhibitory Potency (IC<sub>50</sub>,  $\mu$ M) of Different Classes of HDAC Inhibitors against HDACs 1–11**

Inhibitor	Class	HDAC1	HDAC2	HDAC3	HDAC8	HDAC6	HDAC10	HDAC11	HDAC4	HDAC5	HDAC7	HDAC9
<b>UF010</b> <sup>a</sup>	benzoylhydrazide	0.5	0.1	0.06	1.5	9.1	15.3	44.5	>100	>100	>100	>100
MS-275 <sup>b</sup>	benzamide	0.2	0.5	0.3	>10	5.90	>10	ND	>10	>10	>10	>10
Cpd60 <sup>c</sup>	benzamide	0.001	0.008	0.5	>30	>30	3.4	NA	>30	>30	>30	>30
SAHA	hydroxamic acid	0.06	0.3	0.02	0.8	0.009	0.03	NA	>10	>10	>10	>10
TSA <sup>d</sup>	hydroxamic acid	0.005	0.008	0.01	0.2	0.0007	0.04	0.01	5.0	2.6	1.4	10.4
Romidepsin <sup>e</sup>	cyclic peptide	0.002	0.004	ND	ND	0.8	ND	ND	0.03	ND	ND	ND

ND, not determined.

<sup>a</sup>Dose-response assays were performed in the concentration range of 5 nM to 100  $\mu$ M based on fluorescence assays.

<sup>b</sup>HDAC6 IC<sub>50</sub> was determined in this study; other data from [Laufer et al. \(2013\)](#).

<sup>c</sup>Data from the literature ([Laufer et al., 2013](#); [Schroeder et al., 2013](#)).

<sup>d</sup>HDAC1 and HDAC6 IC<sub>50</sub> data from the literature ([Laufer et al., 2013](#)).

<sup>e</sup>Data from the literature ([Newbold et al., 2013](#)).

bias, and in each instance, the software identified the HDAC active site as the only binding site for **UF010** and analogs. The butyl side chain of these compounds fills a deep hydrophobic (foot) pocket ([Figure S5](#)). An immediate question was if the inhibitors are Zn binders; this modeling analysis indicated in some instances that the hydrazide carbonyl interacted in monodentate manner with the active site Zn, while in others the second (distal) hydrazide nitrogen was within coordination distance of the active site Zn. In no cases was bidentate coordination observed; in many instances, the inhibitors exhibited no interaction whatsoever with the active site Zn. Thus, it appears that the principal mode of binding of this novel class of HDACi is not due to strong interactions with the active site Zn; this distinguishes this class of inhibitors from the vast majority of other known HDAC inhibitors.

### Impact of UF010 on Global Protein Acetylation

In cell-based assays, we exposed HCT116 cells to **UF010** along with other HTS hits (UF003, UF006, UF007, UF008, and UF009; the structures of these hits are shown in [Figure S6A](#)), trichostatin A (TSA) (a hydroxamate), and MS-275 (an aminobenzamide). Data presented in [Figure 1A](#) show that **UF010** consistently induced the accumulation of acetylated histones at all sites we have examined. TSA strongly induced acetylation at some sites but weakly at other sites. In contrast, MS-275 only slightly induced acetylation at several sites but failed to induce acetylation at most sites. This is probably due to the short (1 hr) exposure of the cells to MS-275, as it and other aminobenzamides are known to bind rather slowly to the active site of an HDAC ([Beconi et al., 2012](#); [Chou et al., 2008](#); [Laufer et al., 2013](#)). We also assessed the cellular activities of synthetic **UF010** analogs. In HCT116 cells, their cellular activities are consistent with their in vitro potencies for inhibiting the deacetylation at H4K5, while for H3K18ac, some weak in vitro inhibitors (e.g., **SR-3205**) also notably increased acetylation ([Figure 1B](#)), suggesting that in vitro activities do not exactly reflect cellular effects. Among these analogs, **UF010** and **SR-3205** consistently displayed significant inhibition of cellular HDACs ([Figure 1B](#)).

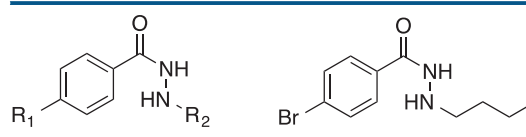
We then assessed the impact of **UF010** on the acetylation of nonhistone proteins. While TSA dramatically increased  $\alpha$ -tubulin acetylation, **UF010** had no effect ([Figures 1C and 1D](#)), even at a high concentration ([Figure S6B](#)). However, **UF010** induced accu-

mulation of acetylated p53 in both HCT116 and A549 cells after exposure to etoposide that inhibits DNA topoisomerase II and induces double-stranded DNA breaks. As expected, etoposide activated the p53 pathway, as indicated by the accumulation of p53 and its transcriptional targets p21 encoded by *CDKN1A* and PUMA encoded by *BBC3* ([Figures 1C and 1D](#)). Both **UF010** and MS-275 also notably stabilized p53 with or without etoposide treatment ([Figures 1C and 1D](#)). HDAC6 (class IIb) is the major tubulin deacetylase ([Hubbert et al., 2002](#); [Matsuyama et al., 2002](#); [Zhang et al., 2003](#)), whereas HDAC1, probably in the context of the NuRD complex, deacetylates p53 ([Contreras et al., 2013](#); [Luo et al., 2000](#)). These data indicate that **UF010** is a class I HDAC-selective inhibitor, in agreement with in vitro biochemical assays ([Table 1](#)).

To identify proteins the acetylation of which is impacted by **UF010** globally, we conducted a proteomic experiment. We found that acetylation of histones H2B, H3, and H4 at most known sites of acetylation was enriched in **UF010**-treated cells ([Table S3](#)). Surprisingly, no acetylated peptides of H2A were detected in our experiment, although both MS-275 and vorinostat were shown to potently induce H2A acetylation ([Choudhary et al., 2009](#)). Acetylated peptides of several other proteins were also enriched ([Table S3](#)). Although these proteins are all known acetylated proteins ([Choudhary et al., 2009](#)), the identified acetylation sites in nucleolin, parathymosin, and PEX14 in **UF010**-treated cells have not been reported thus far ([Table S3](#)). Whereas it is most likely that only the most abundant acetylated peptides were detected in our limited proteomic profiling, these data suggest that **UF010** exerts a distinct impact on global acetylation compared with existing HDAC inhibitors, further supporting the notion that **UF010** possesses unique activities.

### UF010 Is a Competitive HDACi with a Fast-On/Slow-Off Target Binding Mechanism in Cells

The hydroxamic acid and aminobenzamide classes of HDACi occupy the catalytic center of HDACs and display the competitive mechanism of HDAC inhibition ([Chou et al., 2008](#); [Kral et al., 2014](#); [Laufer et al., 2013](#)). We have conducted inhibition kinetic experiments and found that **UF010** is clearly a competitive inhibitor of HDAC2 versus its substrates ([Figure 2A](#)), indicating that **UF010** binds to the substrate pocket of the catalytic core of HDAC2.

**Table 2. SAR of Selected UF010 Analogs<sup>a</sup>**


Compound	UF010		IC <sub>50</sub> Values (μM) <sup>b</sup>				
	R <sub>1</sub>	R <sub>2</sub>	HDAC1	HDAC2	HDAC3	HDAC6	HDAC8
<b>UF010</b>	Br	n-butyl	0.46	1.33	0.19	9.09	2.83
SR-3203	F	n-butyl	13.2	15.1	1.78	ND	ND
SR-3204	-OCF <sub>3</sub>	n-butyl	8.86	9.09	1.35	ND	ND
SR-3205	H	n-butyl	>50	>50	>50	ND	ND
SR-3206	-OMe	n-butyl	1.91	2.52	0.43	ND	ND
SR-3208	-NMe <sub>2</sub>	n-butyl	0.23	0.88	0.12	9.57	0.72
SR-3210	Cl	n-butyl	3.0	3.8	2.5	ND	ND
SR-3302	<i>t</i> -butyl	n-butyl	0.19	1.04	0.07	6.83	0.49
SR-3459	-CH <sub>2</sub> N <sub>3</sub>	n-butyl	0.32	0.53	0.15	10.8	0.89
SR-3212	Br	n-propyl	1.70	3.88	0.22	4.63	ND
SR-3970	Br	n-pentyl	1.87	1.92	0.92	5.73	4.87
SR-3367	Br	n-hexyl	10.27	16.11	20.04	39.1	ND
SR-3213	Br	CH <sub>2</sub> CH <sub>2</sub> Bn	>50	>50	24.18	ND	ND
SR-3297	Br	CH <sub>2</sub> CH <sub>2</sub> ( <i>c</i> -C <sub>5</sub> H <sub>10</sub> )	7.40	7.65	1.08	ND	ND
SR-3364	Br	CH <sub>2</sub> ( <i>c</i> -C <sub>5</sub> H <sub>10</sub> )	8.81	28.45	6.98	ND	ND
SR-3365	Br	CH <sub>2</sub> CH <sub>2</sub> CH <sub>2</sub> ( <i>c</i> -C <sub>5</sub> H <sub>10</sub> )	>50	>50	>50	ND	ND
SR-3298	-NMe <sub>2</sub>	CH <sub>2</sub> ( <i>c</i> -C <sub>5</sub> H <sub>10</sub> )	1.76	3.25	1.67	ND	ND

ND, not determined.

<sup>a</sup>UF010 is an HTS hit. All compounds identified with "SR" numbers are synthetic analogs.

<sup>b</sup>HDAC activity assays were performed using the HDAC-Glo I/II reagents.

The hydroxamates are fast-on/fast-off HDACi, whereas the aminobenzamide HDACi display a slow-on/slow-off HDAC-binding mechanism (Beconi et al., 2012; Chou et al., 2008; Lauffer et al., 2013). To assess how **UF010** might interact with HDACs, we exposed HCT116 cells to various HDACi for 6 hr. The drugs were washed out and the cells were cultured for various lengths of time after drug washout. Consistent with published data (Lauffer et al., 2013), vorinostat induced high levels of histone acetylation (H3K18ac) within 6 hr, and the acetylated histones were quickly reduced to normal levels upon the drug removal (Figure 2B, lanes 7–11). Romidepsin also quickly induced acetylation, and the acetylation levels were stable up to 24 hr (18 hr after drug removal) (Figure 2A, lanes 1–5), suggesting that romidepsin has a slower rate of release from HDACs than vorinostat. The accumulation of histone acetylation induced by the aminobenzamide MS-275 was apparent only at 18 hr after 6 hr exposure, and the acetylated histones were stable up to at least 48 hr (Figure 2B, lanes 12–15), in agreement with a slow-on/slow-off mode of HDAC inhibition (Beconi et al., 2012; Chou et al., 2008; Lauffer et al., 2013). For **UF010**, histone acetylation was induced within 6 hr of exposure, and the levels of induced acetylation were maintained up to 96 hr (Figure 2B, lanes 17–22), suggesting that **UF010** is a fast-on but slow-off inhibitor.

We assessed the HDAC inhibition activity of **UF010**, MS-275, and SAHA in live cell cultures. As shown in Figure 2C, **UF010** exhibited an HDAC inhibition IC<sub>50</sub> of 1.8 μM within minutes after its

addition, and this inhibitory potency remained relatively constant throughout the assay period up to 4 hr. The IC<sub>50</sub> of MS-275 reached the minimum in about 2 hr after drug addition and showed a moderate increase thereafter. The IC<sub>50</sub> of SAHA reached the minimum of ~0.1 μM immediately after drug addition. These data are consistent with the binding kinetics of these inhibitors as observed in drug washout experiments. One surprising finding is that **UF010** is about 5-fold more potent than MS-275 against HDACs in HCT116 (Figure 2C) and HepG2 cells (data not shown). These experiments also indicate that **UF010** quickly penetrates cell membranes and interacts with its cellular targets in cell cultures.

#### HDAC Inhibition Potency of UF010 and Analogs Correlates with their Antiproliferative Effects

To assess the effects of **UF010** and analogs on cancer cell viability, we treated diverse cancer cell lines with **UF010** analogs. In general, **UF010** is less potent to impair the viability of cancer cells than vorinostat or MS-275. For example, the IC<sub>50</sub> values (μM) for killing the colon cancer HCT116 cells were 11.2 for **UF010**, 2.1 for MS-275, and 1.2 for vorinostat. To assess potential roles of HDAC inhibition on cancer cell cytotoxicity, we exposed liver cancer cell line HepG2 to **UF010** and analogs with various in vitro HDAC inhibition potencies. We found that HDAC inhibition potencies of these analogs exhibited an excellent correlation with their cytotoxicity to HepG2 cells (Figure 3A). Indeed, **SR-3208**, which is 2- to 5-fold more potent than **UF010**

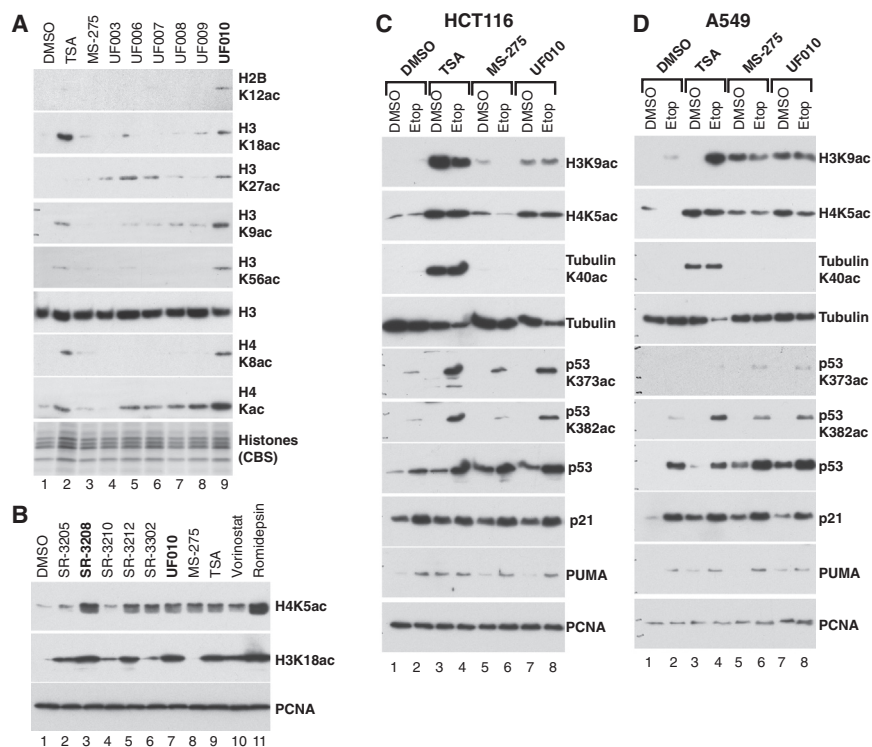


**Figure 1. UF010 Induces the Accumulation of Protein Acetylation**

(A) HCT116 cells were exposed to TSA (0.2  $\mu\text{M}$ ) and other compounds at 2  $\mu\text{M}$  for 1 hr. UF003 and UF006–UF010 are hits identified in the HTS. Histones were extracted and subject to western blotting with antibodies to histones with the indicated modifications or stained with colloidal blue (CBS). The antibodies against H4Kac recognize H4 acetylated at K5, 8, 12, and 16.

(B) The effects of synthetic UF010 analogs on histone acetylation. HCT116 cells were exposed to TSA (0.1  $\mu\text{M}$ ), romidepsin (5 nM), and other compounds at 0.5  $\mu\text{M}$  for 24 hr. The total cell extracts were subject to western blotting with antibodies to histones with the indicated modifications. PCNA was detected as a loading control.

(C and D) HCT116 (C) and A549 (D) cells were exposed to DMSO or etoposide (Etop, 10  $\mu\text{M}$ ) for 6 hr. TSA (0.2  $\mu\text{M}$ ), MS-275, and UF010 (2  $\mu\text{M}$ ) were added 1 hr before cell lysis. The total cell lysates were subject to western blotting with antibodies to the indicated proteins. PCNA was detected as a loading control.

in inhibiting HDACs 1–3, is 3-fold more potent in eliciting cytotoxicity on HepG2 cells. By contrast, **SR-3205**, which did not inhibit HDACs *in vitro*, exerted no growth inhibition for HepG2 cells. Similar effects were also observed in other cancer cell lines (HCT116, colon; MDA-MB-231 and HCC1957, breast cancer; Figures 3B–3D), despite highly variable sensitivities of these cell lines to UF010 analogs. These data suggest that HDAC inhibition appears critical for the UF010 class of HDACi to halt cancer cell growth and proliferation.

UF010 was screened against the NCI-60 panel of cancer cell lines by the National Cancer Institute (NCI) Development Therapeutics Program. It inhibits proliferation of all tested cell lines (including five breast cancer and seven colon cancer cell lines) with a mean  $\text{GI}_{50}$  of 2.94  $\mu\text{M}$ , although sensitivity to this compound varies among these cell lines (Figures 4A and 4B; Figure S7). Cell-cycle analysis using MDA-MB-231 cells exposed to UF010 or vorinostat indicate that UF010 mainly blocked G1/S transition with an increased G1 cell population and a reduced cell population in the S phase in a dose-dependent manner, while vorinostat inhibited G1/S progression at 1  $\mu\text{M}$  but induced a strong G2/M block at 10  $\mu\text{M}$  (Figure 4C). The G2/M checkpoint induced by vorinostat is probably due to a strong DNA-damage response in cells treated with vorinostat (Lee et al., 2010). To assess potential effects of UF010 on cell migration that is associated with metastatic progression, we conducted a wound healing assay. Monolayer MDA-MB-231 cultures were exposed to DMSO, vorinostat (SAHA), or UF010, and then scratched. Cell migration to the denuded areas was assessed. We found that UF010 at 1  $\mu\text{M}$  markedly slowed migration, whereas SAHA did not significantly affect this phenotype (Figure 4D). It is unlikely that possible cross-inhibition of MMPs by UF010 contributes to the inhibition of cell migration, as

SAHA containing the hydroxamic acid warhead that is known to lead to pan-MMP inhibition did not affect cell migration in our experiments. Vorinostat and other hydroxamic acid HDACi have been shown to suppress breast cancer metastases in several preclinical models (Chiu et al., 2013; Huang et al., 2014; Palmieri et al., 2009), although other studies showed that HDACi of the hydroxamic acid class could augment metastatic spread of certain cancer cell lines (Lin et al., 2012).

#### UF010 Activates Tumor Suppression Pathways but Inhibits Oncogenic Signaling

To assess cellular effects of UF010 comprehensively, we treated MDA-MB-231 cells with UF010 at 1  $\mu\text{M}$  for 24 hr and analyzed its impact on global gene expression in comparison with DMSO control using the Affymetrix Human Transcriptome Array 2.0, which allows for the interrogation of transcripts for splicing variants of coding and noncoding genes. The expression of a large number of transcripts was affected due to UF010 treatment, with more downregulated transcripts than upregulated ones overall (Figure 5A). Most of these responsive genes exhibited moderate levels of changes in their mRNA expression. Among the responsive genes that were up or downregulated by 1.5-fold, 115 were upregulated and 68 downregulated (Figure 5A). The changes in gene expression patterns due to UF010 treatment were subject to ingenuity pathway analysis. In the biological function analysis, the most highly affected pathways include the induction of cell death, the suppression of cell-cycle progression, and DNA repair (Figure 5D). In the upstream regulator analysis, UF010 induced the activation of p53 and Rb tumor suppressor pathways but suppressed the MYC, MYCN, and KRAS oncogenic pathways. We showed above that UF010 induced G1 cell-cycle arrest in fluorescence activated cell sorting (FACS) analysis (Figure 4). Concordantly, pathway analysis of our gene expression data revealed that UF010 activated

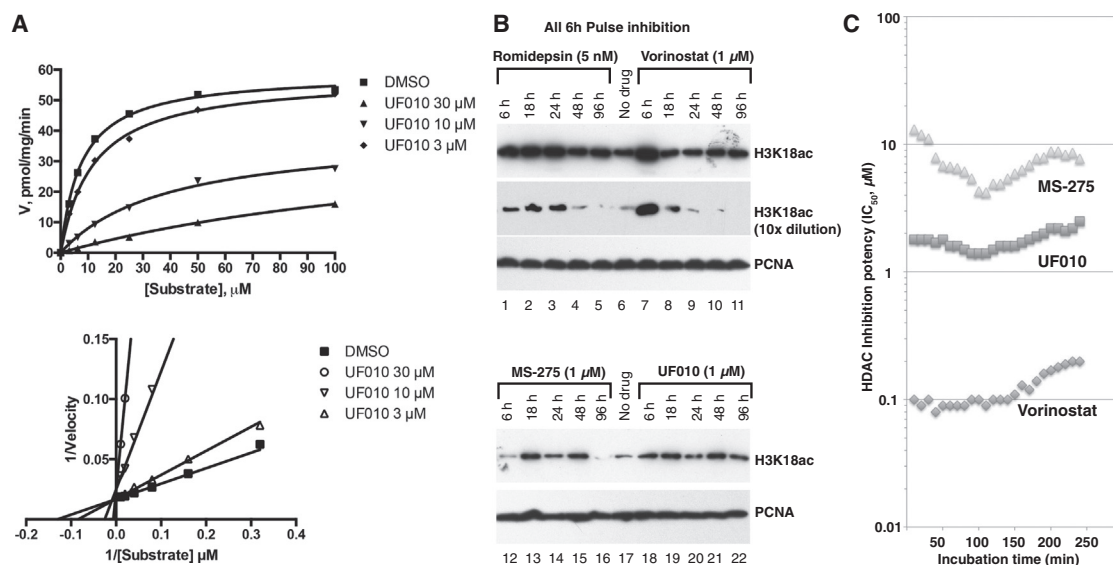


**Figure 2. Mechanisms of HDAC Inhibition by UF010**

(A) Purified HDAC2 was incubated with various concentrations of substrate and **UF010** for various lengths of time. The data were fitted based on the classic Michaelis-Menten kinetics model (top). The  $K_m$  of HDAC2 was determined to be 7.6  $\mu M$  without compound **UF010**. The observed  $K_m$  of HDAC2 was significantly increased in the presence of **UF010**. The Lineweaver-Burke replots of the rate data are shown in the lower panel.

(B) HCT116 cells were pulse treated with the indicated HDACi for 6 hr. The drugs were then washed out, and regular medium was added. The cells were lysed at the indicated times after drug addition. The lysates were subject to western blotting with the indicated antibodies.

(C) HCT116 cell cultures were exposed to various doses of the indicated drugs. HDAC-Glo I/II reagent was added immediately following drug addition. Luminescence was detected 20 min after adding HDAC-Glo I/II reagent, and every 10 min thereafter up to 240 min (4 hr). The HDAC inhibition  $IC_{50}$  was determined and plotted against time.

pathways that promote G1 arrest, while suppressing mechanisms that promote cell-cycle progression (Figure 5B). **UF010**-induced activation of *CDKN1A* encoding p21 was confirmed by quantitative real-time PCR (Figure 5C). Notably, MDA-MB-231 cells express a mutant (R280K) form of p53. Thus, the activation of the p53 pathway by **UF010** is somewhat surprising but could involve partial reactivation of p53 through increasing its acetylation, as **UF010** could indeed increase the levels of acetylated p53 (Figure 1). As expected of an HDACi, this analysis also revealed that **UF010** activated overlapping downstream effectors of the known HDACi, including tributyrin, butyric acid, TSA, and romidepsin (Figure 5D). The inhibition of both HDAC1 and HDAC2 was also revealed in the pathway analysis (Figure 5D), thereby providing an independent validation of **UF010** as a class I-specific HDACi. Interestingly, **UF010** also seems to show overlapping functions with several other drugs, especially genotoxic chemotherapeutics, including cisplatin, camptothecin, doxorubicin, and etoposide (Figure 5D; Table S4). This is consistent with the ability of HDACi to elicit DNA-damage response (Lee et al., 2010).

## DISCUSSION

Potent and selective HDACi serve as powerful tools for probing fundamental biological questions and for ameliorating diverse pathological conditions. Although structurally diverse classes of small-molecule HDACi have been identified, many of the known HDACi feature strong Zn-chelating warheads that could lead to unintended off-target effects. We have identified a novel

group of selective class I HDAC inhibitors with **UF010** as the first-in-class lead compound. This class of HDACi features a novel pharmacophore targeting class I HDACs with a benzoylhydrazide scaffold. Our preliminary SAR studies confirm a tripartite structure of this scaffold with a central  $-C(O)-NH-NH-$  unit flanked by a phenyl group and a short aliphatic chain. The central unit might provide hydrogen-bonding and weak  $Zn^{2+}$ -chelating functionalities, while the flanking hydrophobic groups interact specifically with the hydrophobic pockets in the HDAC catalytic core (Figure S5). Of importance, weaker  $Zn^{2+}$ -chelating warheads in HDACi might reduce off-target activities (Lobera et al., 2013). Our data suggest that **UF010** analogs display a unique HDAC inhibition pharmacology. **UF010** seems more potent in suppressing the deacetylation of histones and p53 than aminobenzamides and less so than hydroxamates possessing a strong  $Zn^{2+}$ -chelating warhead in cell-based assays. Importantly, we found that the HDAC inhibition potencies of **UF010** and analogs correlate directly with their ability to suppress the survival of cancer cells (Figure 3). Bioinformatics analysis of gene expression data also implicates the suppression of HDAC1 and HDAC2 activity by **UF010** (Figure 5D). Thus, HDAC inhibition may underlie their tumor suppressive activity. Notably, **UF010** seems to exert a powerful tumor suppressive effect through activating critical tumor suppressor pathways (e.g., p53 and Rb), while inhibiting several dominant oncogenic mechanisms (e.g., MYC, MYCN, and KRAS), representing novel mechanisms of action for a potential anticancer agent. Our data show that **UF010** is less cytotoxic than both vorinostat and MS-275. Notably, **UF010** is a more potent HDAC inhibitor

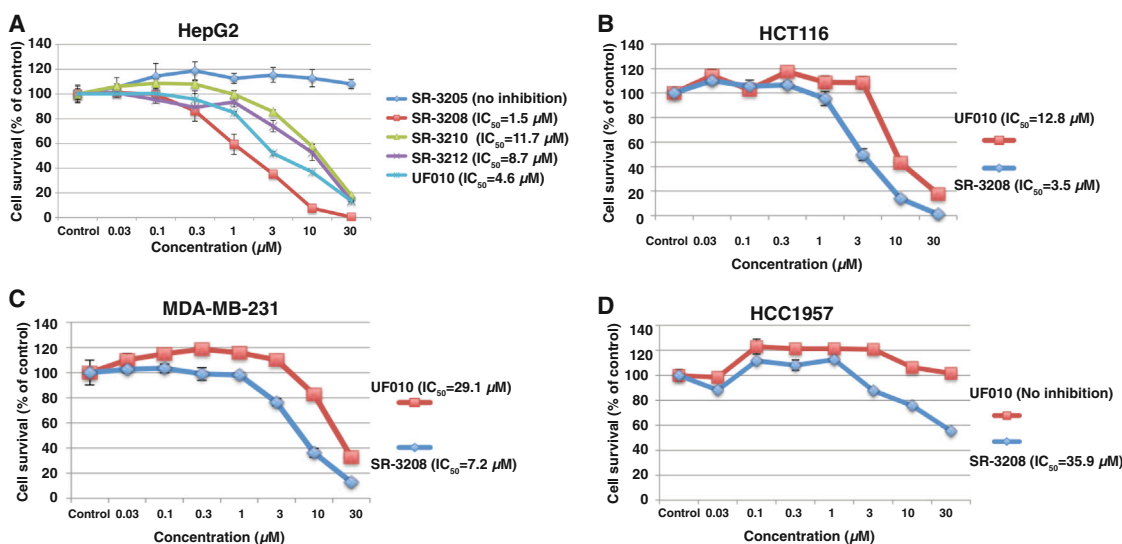


**Figure 3. Suppression of Cancer Cell Viability by UF010 Analogs Correlates with Their HDAC Inhibition Potencies**

(A–D) Hepatocellular carcinoma cell line HepG2 (A), colon cancer cell line HCT116 (B), and breast cancer cell lines MDA-MB-231 (C) and HCC1957 (D) were exposed to DMSO (control) or various doses of **UF010** or an indicated analog. Viable cells were detected at 96 hr after treatment using the CellTiter-Glo assay kit. The fraction of survived cells is plotted against compound concentrations. Error bars show SEM ( $n = 3$ ). The  $IC_{50}$  of each compound was determined using nonlinear regression curve fitting with the Prism 6 software.

than MS-275 in cell-based assays (Figure 2C). These observations suggest that off-target activities of MS-275 might contribute significantly to its cytotoxicity. Regardless, reduced general cytotoxicity for an HDACi may be more desirable for cancer therapy, given the clinical toxicity associated with known HDACi (Martinet and Bertrand, 2011). Furthermore, less toxic compounds might be more suitable for treating diseases such as neurologic conditions and metabolic diseases, as cell death should be avoided in these settings. In preliminary experiments, we found that **UF010** has a half-life of 15.8 hr in cell culture medium containing 10% fetal bovine serum (data not shown), which is similar to that of romidepsin (Furumai et al., 2002). Additional studies will be performed in the future to characterize the pharmacokinetic properties of the **UF010** class of HDACi, after more potent analogs are developed.

HDACs are assembled into several multisubunit complexes such as the Sin3 and NuRD complexes and regulatory subunits in these complexes seem to influence the binding of existing HDAC inhibitors to HDACs. For example, whereas vorinostat exerts potent inhibition of all known HDAC complexes, aminobenzamides seem to show some selectivity against different complexes (Bantscheff et al., 2011). Specifically, aminobenzamides seem inert versus the Sin3 complex. However, we found that **UF010** can inhibit the Sin3 complex (data not shown), further supporting the notion that **UF010** has distinct HDAC inhibitory activities.

In addition to acetylation (C2), lysine residues in histones can also be modified with short-chain *N*-acylation such as propionylation (C3), and butyrylation (C4) (Chen et al., 2007). Histone peptides containing such short-chain acylation can bind to the bromodomains of the bromodomain and extraterminal (BET) family of proteins (e.g., BRD4), although their binding affinity is considerably weaker compared with acetylated peptides (Vollmuth and Geyer, 2010). The short aliphatic chains in the **UF010**

analogs share certain similarity to *N*-acylated lysine, which raises the question as to whether **UF010** analogs might inhibit bromodomains. Although we did not directly test potential activity of **UF010** analogs versus bromodomains *in vitro*, we found that the bromodomain inhibitor I-BET151 synergizes with **UF010** to induce cell death (data not shown), suggesting that **UF010** and I-BET151 have distinct cellular targets.

Pathway analysis of gene expression data revealed that **UF010** exhibits overlapping activities with a number of drugs. Not surprisingly, known HDACi, including tributyrin, butyric acid, TSA, and romidepsin, are identified (Figure 5D), unequivocally confirming that HDACs are the targets of **UF010**. Interestingly, **UF010** seems to share activities with genotoxic chemotherapeutics such as cisplatin, camptothecin, and etoposide. This may stem from the ability of HDACi to elicit DNA-damage response (Lee et al., 2010). This property could also be a consequence of **UF010**-mediated activation of the p53 pathway (Figure 1; Figure 5D). Fulvestrant, a selective estrogen receptor antagonist, was also identified in our bioinformatics analysis (Figure 5D). The class I HDAC-selective HDACi MS-275 (entinostat) has been shown to sensitize ER<sup>+</sup> breast cancer cells to antiestrogen agents, and the combination of entinostat with aromatase inhibitors, which block estrogen synthesis, exhibited improved clinical outcomes for patients with locally advanced or metastatic ER<sup>+</sup> breast cancer in a phase 2 clinical trial (Sabnis et al., 2013; Yardley et al., 2013). Of note, the ER<sup>+</sup> T47D breast cancer cell line is most sensitive to **UF010** among the tested breast cancer cell lines (Figure 4A). It will be of particular interest to determine the effects of **UF010** on ER pathways in breast cancer.

Despite the activation of multiple tumor suppressive pathways in **UF010**-treated MDA-MB-231 cells, they are relatively resistant to **UF010**-mediated apoptosis ( $IC_{50}$  of 29.1  $\mu$ M, Figure 3C). Simultaneous upregulation of stress-response or



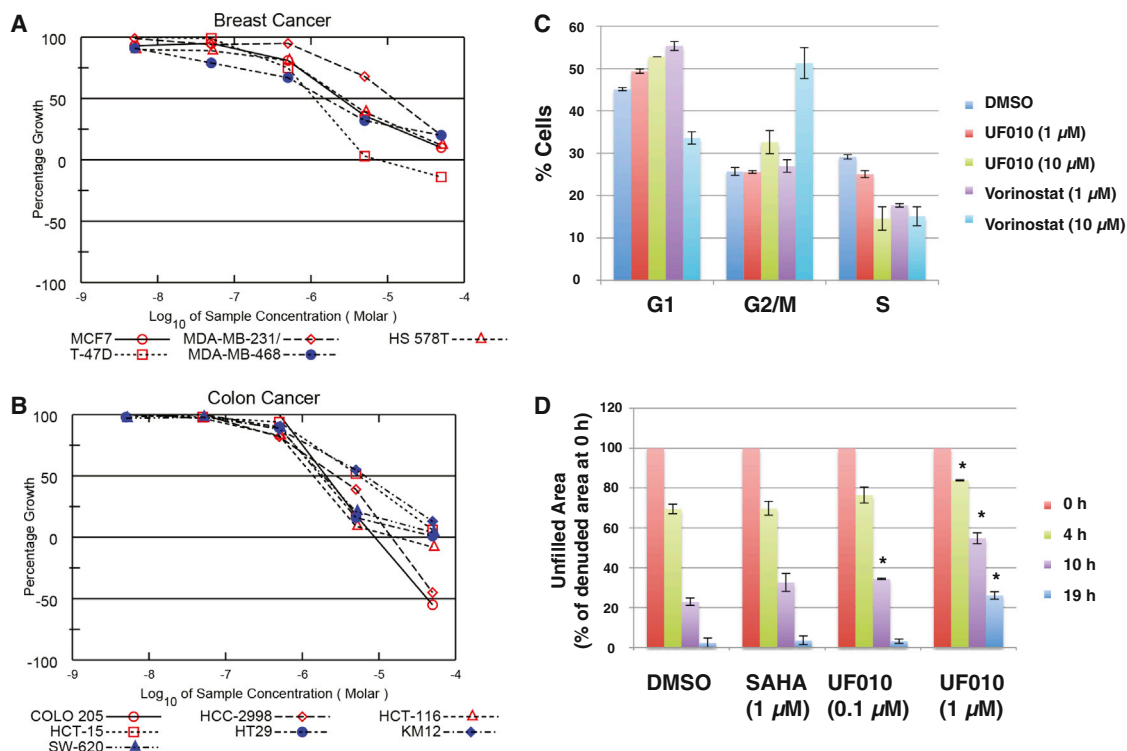


**Figure 4. Antiproliferation Effects of UF010**

(A and B) The indicated breast (A) and colon (B) cancer cell lines in the NCI-60 panel of cancer cell lines were exposed to **UF010** at various concentrations. Percent cell growth relative to the cells seeded before treatment is plotted against the **UF010** concentrations in log scale. For details see Figure S7.

(C) Effects of **UF010** and SAHA (vorinostat) on cell-cycle progression. MDA-MB-231 cells were exposed to DMSO (control) or the indicated doses of **UF010** or SAHA for 24 hr. Cells were then fixed and processed for FACS analysis. Shown are the average values of two experiments along with SEM.

(D) **UF010** suppresses cell migration. MDA-MB-231 cells were exposed to DMSO or the indicated doses of **UF010** or SAHA. At 2 hr after adding a compound, the monolayer cultures were scratched and the denuded areas were photographed at the indicated time points. The uncovered areas were calculated and compared with the initial open areas. Shown are averages  $\pm$  SEM ( $n = 3$ ). \* $p < 0.01$  (versus DMSO treatment).

survival pathways may counteract the apoptotic mechanisms to allow **UF010**-treated cells to survive. The NUPR1 stress-response/chemoresistance pathway was activated in **UF010**-treated MDA-MB-231 cells (Table S4), likely contributing to the survival of **UF010**-treated MDA-MB-231 cells. Indeed, NUPR1 seems to play a critical role in tumor initiation and progression (Cano et al., 2014). In addition, ERK1/2 pathway was also activated (Table S4). These and other cell survival mechanisms are likely to confer resistance to **UF010**. **UF010** combined with inhibitors targeting these survival pathways is predicted to enhance anticancer effects.

In summary, we have identified a new HDACi chemotype that could potentially overcome some of the noted limitations of currently known HDACi. The isotype selectivity coupled with interesting biological activities in suppressing tumor cell proliferation support further preclinical development of the **UF010** class of compounds for potential therapeutic applications.

## SIGNIFICANCE

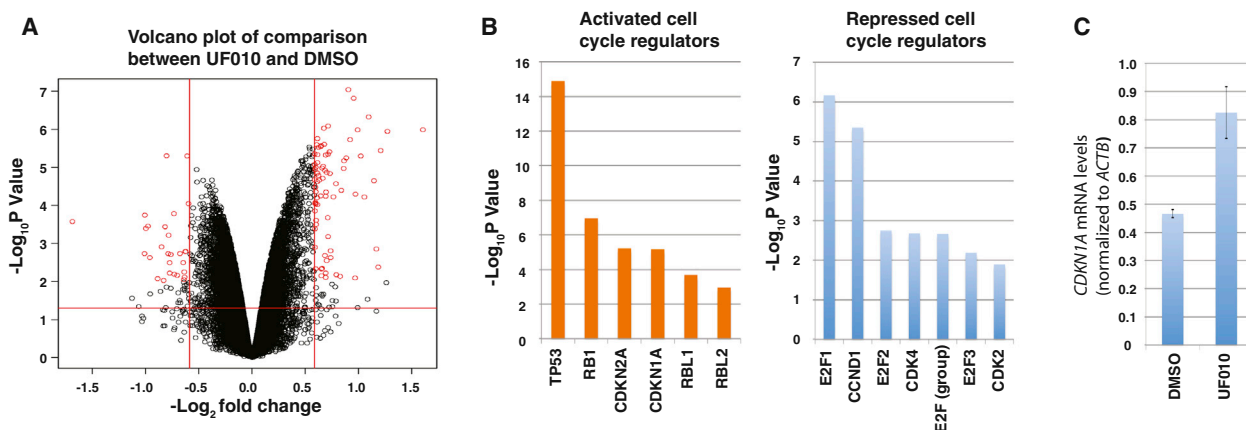
**Small-molecule HDAC inhibitors (HDACi) have therapeutic potentials for treating cancer and other diseases. Three FDA-approved HDACi (vorinostat, belinostat, and romidepsin) are used in clinical anticancer therapy and many other**

**HDACi have been actively tested in clinical trials. Current challenges facing drug development of HDACi include the lack of isoform specificity, undesirable toxicity, and suboptimal therapeutic efficacy against solid tumors. Most HDACi in preclinical or clinical evaluations belong to the hydroxamic acid or aminobenzamide classes. The former class lacks isoform specificity, and the latter shows potentially undesirable pharmaceutical properties. Thus, the identification of HDACi with novel chemical properties and isoform specificity may unleash the considerable therapeutic potential of targeting HDACs. Through an HTS campaign and structure-function relationship study, we have identified a class of HDACi with a previously undescribed benzoylhydrazide scaffold. These compounds are selective to the class I HDACs with nanomolar potencies. These new HDACi inhibited cancer cell proliferation through HDAC inhibition. They activated tumor suppression mechanisms, while inhibiting oncogenic pathways.**

## EXPERIMENTAL PROCEDURES

### HTS Assays

HCT116 cells were stably transduced with a lentiviral vector carrying the firefly luciferase gene under the control of Ad *MLP* (Figure S1). The stable HCT116-*Ad-MLP-Luc* cell line was used for the primary HTS assay (Figure S2).



**D** Perturbation of Selected Cellular Pathways in MDA-MB-231 Cells by UF010

Biological Functions				Upstream Regulators			
Category	Functional annotation	<i>P</i> value	Predicated activation state	Category	Molecule Type	<i>P</i> value	Predicated activation state
Cell growth and proliferation	Proliferation of cells	6.74E-20	Suppressed	TP53	Transcription regulator	1.28E-15	Activated
Cell death and survival	Apoptosis	3.21E-17	Activated	Cisplatin	Chemical drug	3.85E-10	Activated
Gene expression	Transcription of RNA	4.20E-16	Suppressed	Tributyryl (butyrate)	Chemical drug	9.30E-8	Activated
Cell death and survival	Necrosis	3.38E-14	Activated	Rb1	Transcription regulator	1.07E-7	Activated
Cell cycle	Cell cycle progression	2.69E-11	Suppressed	Fulvestrant	Chemical drug	4.41E-7	Activated
DNA replication, recombination and repair	Repair of DNA	4.06E-10	Suppressed	Myc	Transcription regulator	6.93E-7	Suppressed
Cell death and survival	Cell survival	1.01E-9	Suppressed	KRAS	Enzyme	2.11E-5	Suppressed
				Trichostatin A	Chemical drug	1.79E-4	Activated
				MYCN	Transcription regulator	1.40E-3	Suppressed
				Butyric acid	Chemical-endogenous	3.59E-3	Activated
				ERK1/2	Group	3.65E-3	Activated
				Romidepsin	Biologic drug	1.82E-2	Activated
				HDAC1	Transcription regulator	4.02E-2	Suppressed
				HDAC2	Transcription regulator	4.32E-2	Suppressed

**Figure 5. Global Effects of UF010 on Gene Expression**

MDA-MB-231 cells were exposed to DMSO or **UF010** at  $1 \mu\text{M}$  for 24 hr. RNAs were isolated and subject to microarray gene expression profiling.

(A) Volcano plot of gene expression profiles in cell treated with **UF010** in comparison with those treated with DMSO. The two vertical lines in red demark  $\pm 0.585$  of the x axis to indicate genes that were up- or downregulated by 1.5-fold. The red horizontal line indicates  $-1.3$  of the y axis for  $p < 0.05$ .

(B) The cell-cycle regulators that were either activated (left) or suppressed (right) based on the ingenuity upstream regulator analysis. The p value is shown in negative  $\log_{10}$  scale.

(C) qPCR validation of **UF010**-induced upregulation of *CDKN1A* encoding p21. Shown are the average values of three experiments  $\pm$  SEM.

(D) Major pathways affected by **UF010** in MDA-MB-231 cells. The gene expression data were analyzed using ingenuity pathway analysis software as in (B).

Compounds that activated the *MLP-Luc* reporter were tested for in vitro assays for HDAC1 inhibition using the HDAC-Glo I/II reagents (Promega, Figure S4). Selected hits were profiled against all zinc-dependent HDACs at the Reaction Biology Corporation.

### HDAC Activity Assays

Purified HDAC1, HDAC2, and HDAC3 (in complex with the deacetylase activation domain of the human NCOR2 (amino acids 395–498)) were obtained from BPS Bioscience. The enzyme activities were initially tested in a serial dilution of each HDAC using the HDAC-Glo I/II reagents (Promega) according to the manufacturer's protocol. Luminescence was detected using the BMG POLARstar Omega microplate reader. A concentration of each HDAC within the linear response region was used for assaying inhibition of HDAC activity by **UF010** and analogs. Each compound was tested in 10-point dose-response assay in triplicate.  $IC_{50}$  values were determined through linear regression of inhibition data using the Prism 6 software.

### Cell Culture, Viability Assays, and Western Blotting

Cell lines were obtained from ATCC and cultured with DMEM supplemented with 10% bovine calf serum, penicillin to 10 units/ml, and streptomycin to 10  $\mu$ g/ml. For viability assays, 5,000 cells/well were seeded in 96-well plates. Compounds or DMSO control were added 24 hr later. Viability assays were performed 96 hr after compound addition using the CellTiter-Glo reagents (Promega). **UF010** was tested against the NCI-60 panel of cancer cell lines for a one-dose initial screening and the subsequent five-dose titration assays at the Development Therapeutics Program of the NCI (Shoemaker, 2006). For western blotting, cell cultures were exposed to compounds as indicated in relevant figures. Total cell lysates or isolated histones were subjected to SDS-PAGE and western blotting essentially as described (Yang et al., 2013). Antibodies used in this study are described in Table S1.

### Cell-Cycle Analysis and Migration Assay

MDA-MB-231 cells were treated with DMSO, **UF010**, or vorinostat for 24 hr. Cells were fixed and subject to cell-cycle analysis using FACS as described (Li et al., 2011). For cell migration assays, a confluent monolayer culture of MDA-MB-231 cells was pretreated with DMSO, vorinostat, or **UF010** for 2 hr. The cells were scratched with a pipette tip, and the wounded areas were imaged at various time points. The denuded area was quantified using the TScratch software (Geback et al., 2009), and the % areas that were not covered with cells relative to the initial denuded areas were calculated.

### Gene Expression Studies

MDA-MB-231 cells were cultured in a 6-well plate. Cells were exposed in triplicate to DMSO or **UF010** at 1  $\mu$ M final concentration at 24 hr after cell plating. Total RNAs were isolated from the treated cells using the RNeasy kit (Qiagen). The RNAs were then processed for microarray hybridization to the Affymetrix GeneChip Human Transcriptome Array 2.0. Data acquisition, processing, and analysis are described in Supplemental Materials and Methods. For quantitative real-time PCR, the isolated RNAs were reverse transcribed with random hexamers using 2  $\mu$ g of RNA, an RNase inhibitor, and Multiscribe reverse transcriptase (Life Technologies). The resulting cDNAs were diluted and used as input for qPCR using the SYBR green detection method. The qPCR primers are provided in Table S2. The relative levels of gene expression were determined with the  $\Delta\Delta Ct$  method.

### Molecular Docking

Compounds for docking were generated utilizing OPLS-2005 force fields. Crystal structures against which our compounds were evaluated (denoted by the following Protein Data Bank codes: HDAC1, 4BKX; HDAC2, 4LXZ; HDAC3, 4A69; HDAC8, 1W22; HDAC7, 3ZNR) were minimized by Schrödinger's protein preparation wizard to 0.30 Å root-mean-square deviation by adding hydrogens and adjusting bond orders where needed. For details, please see Supplemental Materials and Methods.

### Synthesis of UF010 Analogs

A series of **UF010** analogs were synthesized; they are described in detail in the Supplemental Materials and Methods.

### ACCESSION NUMBERS

The microarray data have been deposited in the Gene Expression Omnibus (GEO) database (<http://www.ncbi.nlm.nih.gov/gds>) under the accession number GSE56823.

### SUPPLEMENTAL INFORMATION

Supplemental Information includes Supplemental Materials and Methods, four tables, and seven figures and can be found with this article online at <http://dx.doi.org/10.1016/j.chembiol.2014.12.015>.

### AUTHOR CONTRIBUTIONS

All authors designed and performed experiments and analyzed the data. Yunfei Wang, R.L.S., C.E.P., P.H., W.R.R., Yuren Wang, and D. Liao wrote the article. H.M., P.H., W.R.R., and D. Liao supervised the study.

### ACKNOWLEDGMENTS

We thank Pierre Baillargeon, Lina DeLuca, and Louis Scampavia for compound management and quality control, Katharine Emery for secretarial assistance, and the NCI Developmental Therapeutics Program for the NCI-60 cell line testing. The work was supported by grants from Bankhead-Coley Cancer Research Program, Florida Department of Health (09BB-11, 09BW-05 and 4BF02) (to D. Liao), and the NIH Roadmap Initiative grant U54MH084512 (to W.R.R.). Yunfei Wang and Dawei Li were supported in part by a scholarship from the China Scholarship Council.

Received: April 18, 2014

Revised: November 14, 2014

Accepted: December 17, 2014

Published: February 19, 2015

### REFERENCES

- Arrowsmith, C.H., Bountra, C., Fish, P.V., Lee, K., and Schapira, M. (2012). Epigenetic protein families: a new frontier for drug discovery. *Nat. Rev. Drug Discov.* *11*, 384–400.
- Bantscheff, M., Hopf, C., Savitski, M.M., Dittmann, A., Grandi, P., Michon, A.M., Schlegl, J., Abraham, Y., Becher, I., Bergamini, G., et al. (2011). Chemoproteomics profiling of HDAC inhibitors reveals selective targeting of HDAC complexes. *Nat. Biotechnol.* *29*, 255–265.
- Beconi, M., Aziz, O., Matthews, K., Moumne, L., O'Connell, C., Yates, D., Clifton, S., Pett, H., Vann, J., Crowley, L., et al. (2012). Oral administration of the pimepic diphenylamide HDAC inhibitor HDACi 4b is unsuitable for chronic inhibition of HDAC activity in the CNS in vivo. *PLoS One* *7*, e44498.
- Bolden, J.E., Peart, M.J., and Johnstone, R.W. (2006). Anticancer activities of histone deacetylase inhibitors. *Nat. Rev. Drug Discov.* *5*, 769–784.
- Bradner, J.E., West, N., Grachan, M.L., Greenberg, E.F., Haggarty, S.J., Warnow, T., and Mazitschek, R. (2010). Chemical phylogenetics of histone deacetylases. *Nat. Chem. Biol.* *6*, 238–243.
- Cano, C.E., Hamidi, T., Garcia, M.N., Grasso, D., Loncle, C., Garcia, S., Calvo, E., Lomber, G., Duseti, N., Bartholin, L., et al. (2014). Genetic inactivation of Nupr1 acts as a dominant suppressor event in a two-hit model of pancreatic carcinogenesis. *Gut* *63*, 984–995.
- Chen, Y., Sprung, R., Tang, Y., Ball, H., Sangras, B., Kim, S.C., Falck, J.R., Peng, J., Gu, W., and Zhao, Y. (2007). Lysine propionylation and butyrylation are novel post-translational modifications in histones. *Mol. Cell. Proteomics* *6*, 812–819.
- Chiu, H.W., Yeh, Y.L., Wang, Y.C., Huang, W.J., Chen, Y.A., Chiou, Y.S., Ho, S.Y., Lin, P., and Wang, Y.J. (2013). Suberoylanilide hydroxamic acid, an inhibitor of histone deacetylase, enhances radiosensitivity and suppresses lung metastasis in breast cancer in vitro and in vivo. *PLoS One* *8*, e76340.

- Chou, C.J., Herman, D., and Gottesfeld, J.M. (2008). Pimelic diphenylamide 106 is a slow, tight-binding inhibitor of class I histone deacetylases. *J. Biol. Chem.* **283**, 35402–35409.
- Choudhary, C., Kumar, C., Gnad, F., Nielsen, M.L., Rehman, M., Walther, T.C., Olsen, J.V., and Mann, M. (2009). Lysine acetylation targets protein complexes and co-regulates major cellular functions. *Science* **325**, 834–840.
- Christensen, D.P., Gysemans, C., Lundh, M., Dahllof, M.S., Noesgaard, D., Schmidt, S.F., Mandrup, S., Birckbak, N., Workman, C.T., Piemonti, L., et al. (2014). Lysine deacetylase inhibition prevents diabetes by chromatin-independent immunoregulation and beta-cell protection. *Proc. Natl. Acad. Sci. USA* **111**, 1055–1059.
- Contreras, A.U., Mebratu, Y., Delgado, M., Montano, G., Hu, C.A., Ryter, S.W., Choi, A.M., Lin, Y., Xiang, J., Chand, H., et al. (2013). Deacetylation of p53 induces autophagy by suppressing Bmf expression. *J. Cell Biol.* **201**, 427–437.
- DasGupta, S., Murumkar, P.R., Giridhar, R., and Yadav, M.R. (2009). Current perspective of TACE inhibitors: a review. *Bioorg. Med. Chem.* **17**, 444–459.
- Day, J.A., and Cohen, S.M. (2013). Investigating the selectivity of metalloenzyme inhibitors. *J. Med. Chem.* **56**, 7997–8007.
- Fass, D.M., Reis, S.A., Ghosh, B., Hennig, K.M., Joseph, N.F., Zhao, W.N., Nieland, T.J., Guan, J.S., Kuhnle, C.E., Tang, W., et al. (2013). Crebinostat: a novel cognitive enhancer that inhibits histone deacetylase activity and modulates chromatin-mediated neuroplasticity. *Neuropharmacology* **64**, 81–96.
- Furumai, R., Matsuyama, A., Kobashi, N., Lee, K.H., Nishiyama, M., Nakajima, H., Tanaka, A., Komatsu, Y., Nishino, N., Yoshida, M., et al. (2002). FK228 (depsipeptide) as a natural prodrug that inhibits class I histone deacetylases. *Cancer Res.* **62**, 4916–4921.
- Geback, T., Schulz, M.M., Koumoutsakos, P., and Detmar, M. (2009). TScratch: a novel and simple software tool for automated analysis of monolayer wound healing assays. *Biotechniques* **46**, 265–274.
- Gojo, I., Jiemjit, A., Trepel, J.B., Sparreboom, A., Figg, W.D., Rollins, S., Tidwell, M.L., Greer, J., Chung, E.J., Lee, M.J., et al. (2007). Phase 1 and pharmacologic study of MS-275, a histone deacetylase inhibitor, in adults with refractory and relapsed acute leukemias. *Blood* **109**, 2781–2790.
- Huang, W.J., Tang, Y.A., Chen, M.Y., Wang, Y.J., Hu, F.H., Wang, T.W., Chao, S.W., Chiu, H.W., Yeh, Y.L., Chang, H.Y., et al. (2014). A histone deacetylase inhibitor YCW1 with antitumor and antimetastasis properties enhances cisplatin activity against non-small cell lung cancer in preclinical studies. *Cancer Lett.* **346**, 84–93.
- Hubbert, C., Guardiola, A., Shao, R., Kawaguchi, Y., Ito, A., Nixon, A., Yoshida, M., Wang, X.F., and Yao, T.P. (2002). HDAC6 is a microtubule-associated deacetylase. *Nature* **417**, 455–458.
- Kral, A.M., Ozerova, N., Close, J., Jung, J., Chenard, M., Fleming, J., Haines, B.B., Harrington, P., Maclean, J., Miller, T.A., et al. (2014). Divergent kinetics differentiate the mechanism of action of two HDAC inhibitors. *Biochemistry* **53**, 725–734.
- Lauffer, B.E., Mintzer, R., Fong, R., Mukund, S., Tam, C., Zilberleyb, I., Flicke, B., Ritscher, A., Fedorowicz, G., Vallerio, R., et al. (2013). Histone deacetylase (HDAC) inhibitor kinetic rate constants correlate with cellular histone acetylation but not transcription and cell viability. *J. Biol. Chem.* **288**, 26926–26943.
- Lee, J.H., Choy, M.L., Ngo, L., Foster, S.S., and Marks, P.A. (2010). Histone deacetylase inhibitor induces DNA damage, which normal but not transformed cells can repair. *Proc. Natl. Acad. Sci. USA* **107**, 14639–14644.
- Li, Q., Zhao, L.Y., Zheng, Z., Yang, H., Santiago, A., and Liao, D. (2011). Inhibition of p53 by adenovirus type 12 E1B-55K deregulates cell cycle control and sensitizes tumor cells to genotoxic agents. *J. Virol.* **85**, 7976–7988.
- Lin, K.T., Wang, Y.W., Chen, C.T., Ho, C.M., Su, W.H., and Jou, Y.S. (2012). HDAC inhibitors augmented cell migration and metastasis through induction of PKCs leading to identification of low toxicity modalities for combination cancer therapy. *Clin. Cancer Res.* **18**, 4691–4701.
- Lobera, M., Madauss, K.P., Pohlhaus, D.T., Wright, Q.G., Trocha, M., Schmidt, D.R., Baloglu, E., Trump, R.P., Head, M.S., Hofmann, G.A., et al. (2013). Selective class IIa histone deacetylase inhibition via a nonchelating zinc-binding group. *Nat. Chem. Biol.* **9**, 319–325.
- Lotsch, J., Schneider, G., Reker, D., Parnham, M.J., Schneider, P., Geisslinger, G., and Doehring, A. (2013). Common non-epigenetic drugs as epigenetic modulators. *Trends Mol. Med.* **19**, 742–753.
- Luo, J., Su, F., Chen, D., Shiloh, A., and Gu, W. (2000). Deacetylation of p53 modulates its effect on cell growth and apoptosis. *Nature* **408**, 377–381.
- Marks, P.A. (2010). The clinical development of histone deacetylase inhibitors as targeted anticancer drugs. *Expert Opin. Investig. Drugs* **19**, 1049–1066.
- Martinet, N., and Bertrand, P. (2011). Interpreting clinical assays for histone deacetylase inhibitors. *Cancer Manag. Res.* **3**, 117–141.
- Matsuyama, A., Shimazu, T., Sumida, Y., Saito, A., Yoshimatsu, Y., Seigneurin-Berny, D., Osada, H., Komatsu, Y., Nishino, N., Khochbin, S., et al. (2002). In vivo destabilization of dynamic microtubules by HDAC6-mediated deacetylation. *EMBO J.* **21**, 6820–6831.
- Muller, B.M., Jana, L., Kasajima, A., Lehmann, A., Prinzler, J., Budczies, J., Winzer, K.J., Dietel, M., Weichert, W., and Denkert, C. (2013). Differential expression of histone deacetylases HDAC1, 2 and 3 in human breast cancer—overexpression of HDAC2 and HDAC3 is associated with clinicopathological indicators of disease progression. *BMC Cancer* **13**, 215.
- New, M., Olzscha, H., and La Thangue, N.B. (2012). HDAC inhibitor-based therapies: can we interpret the code? *Mol. Oncol.* **6**, 637–656.
- Newbold, A., Matthews, G.M., Bots, M., Cluse, L.A., Clarke, C.J., Banks, K.M., Cullinane, C., Bolden, J.E., Christiansen, A.J., Dickins, R.A., et al. (2013). Molecular and biologic analysis of histone deacetylase inhibitors with diverse specificities. *Mol. Cancer Ther.* **12**, 2709–2721.
- Nuti, E., Casalini, F., Santamaria, S., Gabelloni, P., Bendinelli, S., Da Pozzo, E., Costa, B., Marinelli, L., La Pietra, V., Novellino, E., et al. (2011). Synthesis and biological evaluation in U87MG glioma cells of (ethynylthiophene)sulfonamide-based hydroxamates as matrix metalloproteinase inhibitors. *Eur. J. Med. Chem.* **46**, 2617–2629.
- Ononye, S.N., van Heyst, M., Falcone, E.M., Anderson, A.C., and Wright, D.L. (2012). Toward isozyme-selective inhibitors of histone deacetylase as therapeutic agents for the treatment of cancer. *Pharm. Pat. Anal.* **1**, 207–221.
- Palmieri, D., Lockman, P.R., Thomas, F.C., Hua, E., Herring, J., Hargrave, E., Johnson, M., Flores, N., Qian, Y., Vega-Valle, E., et al. (2009). Vorinostat inhibits brain metastatic colonization in a model of triple-negative breast cancer and induces DNA double-strand breaks. *Clin. Cancer Res.* **15**, 6148–6157.
- Sabnis, G.J., Goloubeva, O.G., Kazi, A.A., Shah, P., and Brodie, A.H. (2013). HDAC inhibitor entinostat restores responsiveness of letrozole-resistant MCF-7Ca xenografts to aromatase inhibitors through modulation of Her-2. *Mol. Cancer Ther.* **12**, 2804–2816.
- Schroeder, F.A., Lewis, M.C., Fass, D.M., Wagner, F.F., Zhang, Y.L., Hennig, K.M., Gale, J., Zhao, W.N., Reis, S., Barker, D.D., et al. (2013). A selective HDAC 1/2 inhibitor modulates chromatin and gene expression in brain and alters mouse behavior in two mood-related tests. *PLoS One* **8**, e71323.
- Shoemaker, R.H. (2006). The NCI60 human tumour cell line anticancer drug screen. *Nat. Rev. Cancer* **6**, 813–823.
- Smith, B.C., Hallows, W.C., and Denu, J.M. (2008). Mechanisms and molecular probes of sirtuins. *Chem. Biol.* **15**, 1002–1013.
- Vollmuth, F., and Geyer, M. (2010). Interaction of propionylated and butyrylated histone H3 lysine marks with Brd4 bromodomains. *Angew. Chem. Int. Ed. Engl.* **49**, 6768–6772.
- Wagner, F.F., Weiwer, M., Lewis, M.C., and Holson, E.B. (2013). Small molecule inhibitors of zinc-dependent histone deacetylases. *Neurotherapeutics* **10**, 589–604.
- Wilson, A.J., Byun, D.S., Popova, N., Murray, L.B., L'Italien, K., Sowa, Y., Arango, D., Velcich, A., Augenlicht, L.H., and Mariadason, J.M. (2006). Histone deacetylase 3 (HDAC3) and other class I HDACs regulate colon cell maturation and p21 expression and are deregulated in human colon cancer. *J. Biol. Chem.* **281**, 13548–13558.

- Yang, X.J., and Seto, E. (2008). The Rpd3/Hda1 family of lysine deacetylases: from bacteria and yeast to mice and men. *Nat. Rev. Mol. Cell Biol.* **9**, 206–218.
- Yang, H., Pinello, C.E., Luo, J., Li, D., Wang, Y., Zhao, L.Y., Jahn, S.C., Saldanha, S.A., Planck, J., Geary, K.R., et al. (2013). Small-molecule inhibitors of acetyltransferase p300 identified by high-throughput screening are potent anticancer agents. *Mol. Cancer Ther.* **12**, 610–620.
- Yardley, D.A., Ismail-Khan, R.R., Melichar, B., Lichinitser, M., Munster, P.N., Klein, P.M., Cruickshank, S., Miller, K.D., Lee, M.J., and Trepel, J.B. (2013). Randomized phase II, double-blind, placebo-controlled study of exemestane with or without entinostat in postmenopausal women with locally recurrent or metastatic estrogen receptor-positive breast cancer progressing on treatment with a nonsteroidal aromatase inhibitor. *J. Clin. Oncol.* **31**, 2128–2135.
- Zhang, Y., Li, N., Caron, C., Matthias, G., Hess, D., Khochbin, S., and Matthias, P. (2003). HDAC-6 interacts with and deacetylates tubulin and microtubules in vivo. *EMBO J.* **22**, 1168–1179.